Reports on Geodesy and Geoinformatics, 2024, Vol. 117, pp. 11–20

DOI: 10.2478/rgg-2024-0002
Received: 4 December 2023 / Accepted: 28 December 2023
Published online: 2 February 2024

ORIGINAL ARTICLE

A comparative analysis of the performance of various GNSS positioning concepts dedicated to precision agriculture

Wiktoria Zofia Kowalczyk [1] and Tomasz Hadas [1*]

[1]Institute of Geodesy and Geoinformatics, Wrocław University of Environmental and Life Sciences, C.K. Norwida 25, 50-375 Wrocław, Poland

[*]tomasz.hadas@upwr.edu.pl

Abstract

Automated guidance systems for precision agriculture rely on Global Navigation Satellite Systems (GNSS) and correction services for high accuracy and precision in field operations. This study evaluates the performance of selected GNSS positioning services for precision agriculture in a field experiment. We use three correction services: SF1, SF3, and RTK, which apply varying positioning concepts, i.e., Wide Area Differential GNSS, Precise Point Positioning, and Real-Time Kinematics, respectively. The tractor is autonomously steered along multiple predefined paths located in open-sky areas as well as near the heavy tree cover. The reference route of the vehicle is determined by classical surveying. Tractor trajectories, a SF1 and SF3 corrections, are shifted from predefined straight paths, unlike in the case for RTK. Offsets of up to several decimeters are service- and area-specific, indicating an issue with the stability of the reference frame. Additionally, the varying performance of the correction services implies that environmental conditions limit the precision and accuracy of GNSS positioning in precision agriculture. The pass-to-pass analysis reveals that SF1 improves the declared accuracy, while SF3 is less reliable in obstructed areas. RTK remains a stable source for determining position. Under favorable conditions, the pass-to-pass accuracy at 95% confidence level is better than 11.5 cm, 8.5 cm, and 4.5 cm for SF1, SF3, and RTK, respectively. In the worst-case scenario, the corresponding accuracies are: 25.5 cm, 65.5 cm, and 22.5 cm.

Key words: Precision agriculture, GNSS, Starfire, automated guidance system

1 Introduction

Precision agriculture (PA), practiced by a growing number of farmers (Coyne et al., 2003), involves the application of a set of technologies that allow them to optimize work time and save costs while increasing farm productivity and improving the quality of yields. The PA cycle begins with the collection of soil samples from various zones in the field to analyze soil abundance (Mawardi et al., 2018; Huuskonen and Oksanen, 2018). For this purpose, available soil-type maps are used, or prepared using, among others, electromagnetic sensors. The results are presented on soil abundance maps, which are the basis for the farmers to use Variable Rate Technology (VRT). A practical implementation of VRT in agricultural treatments is Variable Rate Application (VRA). Performing field-adapted treatments is possible using VRA prescription maps, and thus the use of chemical pesticides and fertilizers is minimized (He, 2022). Inadequate application rates can result in stunted plant growth, root system damage, and soil degradation (Onyango et al., 2021). Conversely, using properly balanced and adjusted doses, improves the plant condition, and helps avoid excess chemicals remaining in soil or watercourses. To be able to meet the above-mentioned objectives, PA-dedicated systems allow farmers to use a number of functions, such as section control (Luck et al., 2010). This VRA map-based tool reduces skipping and overlapping during such treatments as: seeding, fertilizing, or spraying (Lange and Peake, 2020). Overlapping is further limited by automated guidance systems, which reduce the need for manual steering by the operator, allowing for autonomous, hands-free work. It benefits farms by optimizing input fuel costs and increasing machine's efficiency (Harbuck et al., 2006) also making it possible to operate large vehicles with centimeter accuracy (Lange and Peake, 2020).

The automated guidance system works with a Global Navigation Satellite Systems (GNSS) receiver and uses a controller in the hydraulic system as well as a steering sensor (Esau et al., 2021). The tractor is either integrated with the system in a factory or requires a purchase of dedicated hardware to upgrade to an automated guidance system (Kim et al., 2013; Keicher and Seufert, 2000). The accuracy that the machine can achieve in an autonomous ride depends on many factors, such as: correction services for GNSS positioning, terrain conditions, and machine configuration (Huyghebaert et al., 2013). During the steering optimization setup, the farmer can specify the steering system's response speed and guidance sensitivity. Autoguidance systems include different types of modules for terrain compensation (Adamchuk, 2008). Before performing the agricultural treatment, farmers calibrate the vehicle so that pitch, roll, and yaw can be detected during the ride (Bak and Jakobsen, 2004). Terrain compensation increases the effectiveness of autonomous guidance and facilitates accurate positioning. This is especially important for farmers whose crops are on sloping terrain or rough ground. Automatically steered tractors while on the field either use machine vision or are guided on paths defined prior to the ride (Keicher and Seufert, 2000; Bell, 2000). Not only do the systems allow the tractor to follow (mostly used) straight paths but also curves, arcs, or spirals (Reid and Searcy, 1987). The first approach to auto-guidance requires the use of cameras and digital analysis (Pini et al., 2020), while the second one – the satellite-based position.

A key role in the practice of PA is the precise determination of the machine's position during work using GNSS (Perez-Ruiz et al., 2012). It has played a significant role in PA since as early as the mid-1990s. A pioneer Differential GNSS (DGNSS) service has been offered by John Deere's Starfire 1 (SF1) with a global accuracy of about 1m, followed by the Trimble OmniSTAR Virtual Base Station (VBS) with comparable accuracy. Over the past two decades, GNSS has become easier available, providing more constellations, satellites, frequencies, and corresponding products for more accurate positioning (Montenbruck et al., 2020). This technology has become an integral part of modern farms. PA has evolved along with GNSS, placing greater demands on navigation systems (Tran et al., 2020). Some manufacturers have modernized systems by switching from DGNSS to Precise Point Positioning (PPP) (Zumberge et al., 1997),a technique that is widely used in PA as well as naval and aviation applications. The PPP determines absolute and precise positions based on carrier phase and pseudorange observations at two or more frequencies combined with precise satellite orbits and clock corrections. In addition, the undoubted advantage of the technique is that no reference station is required (Guo et al., 2018). It has been implemented in NovAtel TerraStar, John Deere StarFire, and Trimble OmniSTAR, among others, all of which are subscription services. PA navigation manufacturers often specify the accuracy of their systems with the term "pass-to-pass accuracy" (International Organization for Standardization, 2010). Upon completing a pass in the field and returning to the original position based on a GNSS measurement, an observable discrepancy exists. Pass-to-pass accuracy is a parameter in which bias errors between consecutive passes are used to assess the consistency of positioning along the path. The most advanced global services, i.e., TerraStar-C, StarFire SF3, and OmniSTAR G2, provide pass-to-pass accuracy (95% confidence level) of 3 cm, 3 cm, and 1–2 in, respectively.

In PA, the GNSS receivers are typically mounted on the top of a tractor, usually at the front or in the middle of the cab's roof. The receiver is selected following the user's expectations, the farm's specific requirements, as well as terrain conditions of their fields (Catania et al., 2020). There are many manufacturers who offer equipment with different levels of accuracy, ranging from 50 cm to 2.5 cm (Stombaugh, 2018). The receivers can determine positions using a variety of correction services: the basic ones offered together with the receiver purchase, and those that require an additional subscription and which are providing superior performance. In PA, PPP corrections are typically delivered via geostationary satellites, delivering high accuracy and precision (Radočaj et al., 2023). Positioning using the Real Time Kinematics (RTK) technique is possible for most receivers and is now increasingly popular among farmers. The main disadvantage of the technique is that it requires a connection with a reference station using the radio or the internet. Since the minimum distance from the reference station is required, many farmers set up their own base stations. The advantage of the RTK technique is that it achieves a single-centimeter accuracy, expected by the PA community. Despite the maturity of satellite positioning, the precision and accuracy are limited by the signal nature and satellite products. The latter are critical for the PPP and they propagate the global reference frame. In contrast, for RTK, it is the base station that defines the local coordinate system (Huisman and de Ligt, 2023). Moreover, GNSS signals are interfered with by the propagation medium (Karaim et al., 2018). While most of the error sources cancel out in the RTK technique or are modeled in the PPP technique, signal reflections from surrounding structures or the ground, so-called multipaths, remain major error sources. A variety of signal integrity monitoring techniques exist and they are continuously evolving, but none of them has been working sufficiently effectively in all cases yet (Zabalegui et al., 2020). Multipath, as well as signal blockage, can degrade or even prevent positioning with GNSS. This requires switching to manual steering which leads to disruption of the precise cultivation continuity (Cheein and Carelli, 2013).

This study evaluates the positioning accuracy of selected GNSS services for PA under the conditions of a field experiment. We used the RTK technique and two correction services: SF1 and SF3, provided by Starfire, to autonomously steer a tractor along multiple predefined paths. The reference route of the vehicle was determined by classical surveying. The results are discussed and confronted with accuracies specified by the manufacturer.

2 Methods

2.1 Test Area

The experiment was conducted in south-western Poland on March 21st, 2023, and lasted approximately 2 hours in moderate weather conditions. The test area is approximately 10 ha of flat field, and its southwest side borders a dense forest. The the tractor's routes were designed both in an area with open-sky conditions and where the GNSS signal is often lost, leading to inaccurate positioning (Figure 1). We designed eight straight paths (named: AB, CD, EF, GH, IJ, KL, MN, OP) with known start and finish points and one circular path with a known center point (R) and the radius. The straight paths were 70 m long and the offset between the paths for each pair was 20 m. The radius of the circular path was 20 m

The John Deere 7730 tractor followed the paths with the defined speed of 8 km/h guided by SF1, SF3, and RTK services for automatic steering. The AB, CD, and R paths, designed in

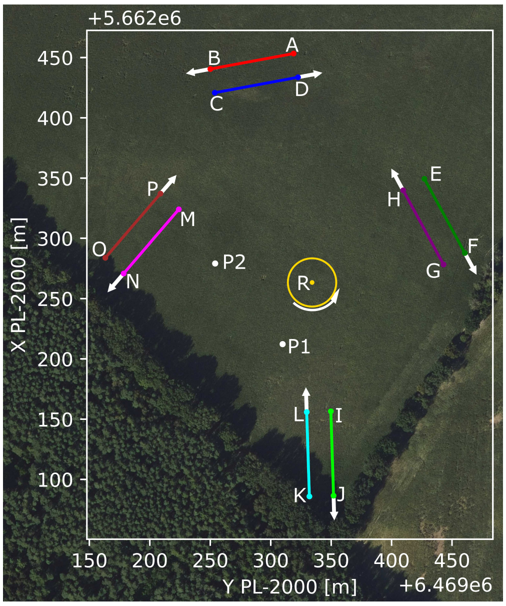

Figure 1. Test area with the designed paths

Table 1. Coordinates and sigma uncertainty of estimated coordinates for P1 and P2, PL-2000 (18°E) reference frame

	Point:	
	P1	**P2**
X [m]	5662212.904	5662279.545
σX [mm]	1.2	1.2
Y [m]	6469309.666	6469253.867
σY [mm]	1.2	1.2
H [m]	148.836	148.852
σH [mm]	2.9	2.9

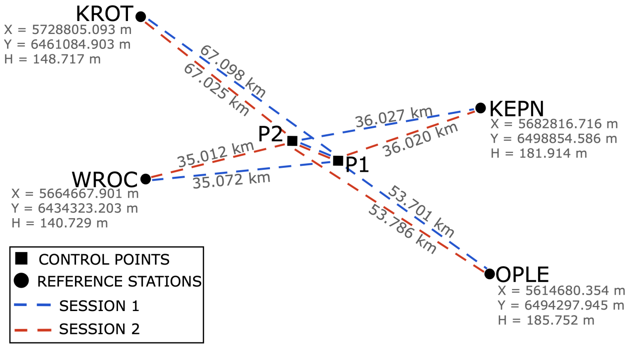

Figure 2. GNSS baselines for the constrained LSA of the P1 and P2 positions

Figure 3. Horizontal and vertical offsets between the GNSS antenna and the retroreflector

an open-sky area, were used once per correction service, while three runs per service were performed on other paths to increase the reliability of the results. The total distance covered by the tractor was 4.2 km for straight paths and approximately 377 m for circular paths. The total number of positions determined by the receiver was 37226, among which 10300 positions were paths of interest. The interval of the measurement was 0.2 s. Points excluded from further analysis were the positions of the tractor determined with manual steering, while driving between pairs of interest as well as making U-turns, since the tractor cannot turn automatically.

2.2 Reference Path

We used surveying techniques to determine the tractor's reference route. On March 13th 2023, two control points: P1 and P2, were established using static GNSS positioning. Trimble R6 receivers took simultaneous measurements during two 30-minute sessions. We downloaded the corresponding multi-GNSS observations from four nearest reference stations (WROC, KEPN, OPLE, and KROT) of the Polish GBAS, i.e., ASG-EUPOS (www.asgeupos.pl). The station positions were defined in the ETRF2000 at epoch 2011.0. We use precised multi-GNSS orbits from the Centre of Orbit Determination (CODE). We conducted a constrained least squares adjustment (LSA) of GNSS baselines (Figure 2) using the Leica Infinity software. The estimated coordinates and errors of point positions after LSA are presented in Table 1.

We used the Trimble S5 robotic total station to determine the vehicle's reference route with a 1 s measurement interval. P1 was used for the total station, and P2 was used as a reference point. The 360-degree prism was installed in the center of the cab roof behind the GNSS receiver with a horizontal and vertical offset, which were measured directly with a ruler (Figure 3). Using the Auto Lock function, the instrument automatically tracked the prism as the tractor followed the paths. The total station registered 2859 points, from which 1964 points were paths of interest.

2.3 GNSS Data

We used a dual-frequency John Deere Starfire 6000 receiver, which tracks GPS and GLONASS satellites. The receiver was mounted on the front of the tractor's cab roof (Figure 3). The auto-guidance system drove the vehicle along predefined paths. All steering optimization settings had been set to default for the duration of the test. The tractor had been calibrated with an integrated Terrain Compensation Module (TCM) prior to the experiment.

The GNSS receiver provided pseudorange P and carrier-phase L observations:

$$P^s_{r,i} - \rho^s_{0,r} = \mathbf{e}^s_r \cdot \delta\mathbf{X}_r + c\left(\delta t_r - \delta t^s\right) + T^s_r + \frac{f_1^2}{f_i^2} \cdot I^s_{r,1} \quad (1)$$

$$L^s_r - \rho^s_{0,r} = \mathbf{e}^s_r \cdot \delta\mathbf{X}_r + c\left(\delta t_r - \delta t^s\right) + T^s_r - \frac{f_1^2}{f_i^2} \cdot I^s_{r,1} + \lambda_i \cdot N^s_i \quad (2)$$

Table 2. Characteristics of the corrections services

Service	Pass-to-pass accuracy [cm]	Pull in time [min]
SF1	±15	<10
SF3	± 3	<30
RTK	± 2.5	<1

with

$$\mathbf{e}_r^s = \left[\frac{X_r - X^s}{\rho_0^s}, \frac{Y_r - Y^s}{\rho_0^s}, \frac{Z_r - Z^s}{\rho_0^s}\right] \quad (3)$$

$$\delta\mathbf{X}_r = \left[\delta X_r, \delta Y_r, \delta Z_r\right]^T \quad (4)$$

where:
i – signal (frequency) indicator,
$\rho_{0,r}^s$ – calculated distance between the receiver r and satellite s,
c – speed of light,
δt_r and δt^s – receiver and satellite clock offsets,
T – troposphere delay,
f_i – frequency of the i-th signal,
I_1 – ionosphere delay for f_1,
λ – wavelength,
N – the carrier phase ambiguity,
(X^s, Y^s, Z^s) – satellite coordinates,
(X_r, Y_r, Z_r) – a-priori receiver coordinates for which the increments $\delta\mathbf{X}_r$ are estimated.

The GNSS receiver offers three corrections services: SF1, SF3, and RTK, which represent different positioning concepts: Wide-Area Differential GNSS (WADGNSS), PPP, and RTK, respectively (https://www.deere.com/en/). The service performance, as specified by the manufacturer, is shown in Table 2. These values are derived for 95% confidence intervals over 15-minute periods in perfect atmospheric and satellite conditions, after pull in time, i.e., when convergence is reached, with the ground conditions as well as automatic-steering-related mechanical errors not taken into account. Despite numerous variations of the aforementioned positioning concepts, the following description applies to the algorithms implemented by John Deere in the Starfire 6000 receivers.

WADGNSS (Kee et al., 1991) uses broadcast ephemeris, fixed positions of tens of worldwide GNSS stations, and dual-frequency pseudorange and carrier-phase observations from these stations. The master station smooths carrier-phase observations to reduce local errors and generates vector corrections for the ionosphere delay, troposphere delay, and the satellites ephemeris and clock errors. The normalized pseudoranges and normalized differences of carrier phases are weighted and form satellite-specific pseudorange corrections (PC) and rate corrections (PRC), respectively. The PC and PRC are provided for all satellites in view and are applied on the user's side.

The PPP technique uses dual or multi frequency observations, combined with precise satellite orbit and clock products, which has to be transmitted to the user, together with the satellite signal biases. Moreover, signal propagation errors and geophysical models are closely considered, so that the $\rho_{0,r}^s$ is already corrected for ocean and solid-earth tides, troposphere hydrostatic delay, phase wind-up, satellite and receiver antenna phase center offset and variations (Schönemann, 2014). The troposphere wet delay and ionosphere delay are estimated on the user's side, and carrier phase ambiguities are resolved as integers under the availability of carrier phase biases.

The RTK uses broadcast ephemeris, a single or multi-GNSS pseudorange and carrier-phase observations from the user receiver and nearby reference receiver, for which the coordinates are fixed. By forming double-differences of observations (using observations from two receivers to two satellites), both clock offsets, satellite orbit inaccuracy, signal biases, troposphere and ionosphere delays, and geophysical effects are all eliminated, leading to a simplified observation model, and an almost instantaneous determination of integer ambiguities is possible (Teunissen and Khodabandeh, 2015).

Table 3. Subset of NMEA parameters used

Sentence	Content used	Format / Unit
GGA	Latitude, Longitude Time Number of satellites	[ddmm.mmmm] [hhmmss.sss] [-]
GSA	PDOP, HDOP, VDOP	[-]
VTG	Heading Velocity	[degrees] [km/h]

We analyzed data acquired by the GNSS receiver using all three corrections services. The data were supplied in the NMEA 0183 format, but only a subset of parameters (Table 3) was subject of a further analysis.

2.4 Reference Frame Unification

We performed a series of transformations between the reference frames to unify the data from the two measurement sources. As the coordinates of ASG-EUPOS stations were in the PL-ETRF2000 reference frame, epoch 2011.0, the coordinates acquired during the survey with a total station were in the same reference frame and epoch. They were directly transformed into the PL-2000 (18°E) frame. Thus, the horizontal and vertical components were decomposed. The GNSS coordinates acquired with the Starfire receiver were in the ITRF2008, epoch 2018.0. Using the transformation parameters between ITRF2008 and ETRF2000, propagated to epoch 2018 with parameter rates, we conducted a 14-parameter transformation and obtained coordinates in ETRF2000, epoch 2018. Due to the missing ETRF2000 velocities of the measured points, we used the velocity of the nearby EPN station, i.e., WROC, and propagated the coordinates to ETRF2000 epoch 2011, which allowed for a transformation into the PL-2000 (18°E) frame, which completed the unification of coordinate reference frame for further analysis.

3 Results

3.1 Surveying conditions

We used NMEA data to investigate the Position Dilution of Precision (PDOP) values during the experiment (Figure 4) to determine the impact of satellite geometry with respect to the receiver on the performance of GNSS positioning – higher values indicated lower precision. In open-sky areas, PDOP remained between 1.0 and 1.2, indicating good geometry of navigation satellites. However, near points F, G, J, and N, as well as those along the OP path, the PDOP increased to 1.6–1.8, reflecting the presence of tree cover. Extreme values of PDOP, exceeding 3.0, were observed when the tractor made a southbound pass and turned under the cover of trees near point K.

The receiver dynamics and the corresponding satellite geometry characteristics are further highlighted in Figure 5. The number of satellites in view varied from 10 to 22. Greater satellite availability was associated with lower DOP values, indicating improved precision in both horizontal and vertical positioning. There were several periods with 10–12 visible satellites,

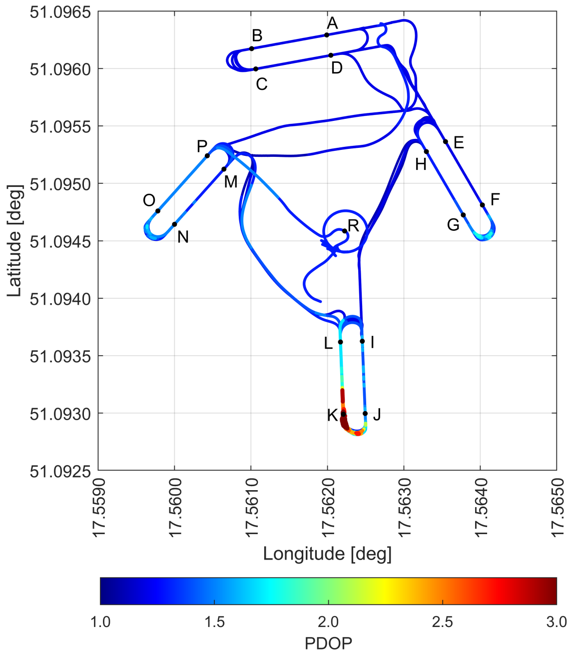

Figure 4. Variability of PDOP value in the test area

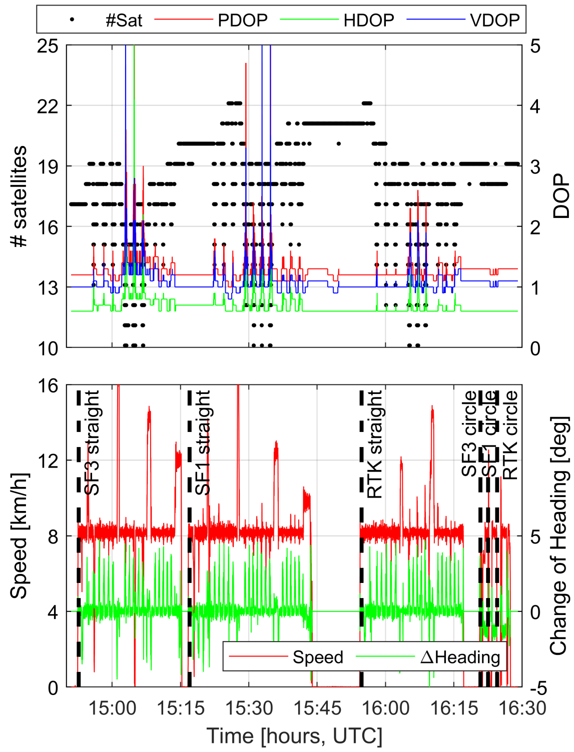

Figure 5. Number of visible satellites DOP values (top), tractor speed and change of heading (bottom) during the test

and the DOP indicators rose to a maximum of 5.0. These events occurred repetitively along the KL path and both SF1 (approximately 15:05 to 15:10) and SF3 (15:30–15:35) services. For the RTK, the DOP values also increased while driving along the KL path (ca. 16:05 to 16:10), but remained below 2.6, despite the similarly low number of satellites in view. Despite the varying measurement conditions, tractor speed while autosteering along all straight and circular paths oscillated around the preset 8 km/h with all three correction services. Higher and lower speed occurred when driving in manual steering mode. Importantly, DOP values remained below 3.0 throughout all autosteering operations.

3.2 Internal Validation

We refer to the GNSS data source as internal. We analyzed the distances of the points measured with the Starfire 6000 receiver from a predefined path: (a) a straight line defined by the coordinates of the start and finish points, or (b) a circle defined by the coordinates of the central point and the radius. In scenario (b), due to the significant south-east offset of the measured path, we used least squares adjustment to fit a circle into GNSS points and determine point R' as its center. For each correction service and each path individually, we calculated the standard deviation (SD) of distances as a measure of precision and root mean square error (RMSE) as a measure of accuracy. We conducted all analyses and visualizations using the Python programming language.

We observed the consistency of tracks for each path and service (Figure 6). Typically, the differences did not exceed 5 cm. However, for many paths we detected a systematic shift with respect to the corresponding predefined path, ranging from approximately -15 cm (GH) to +15 cm (EF). Additionally, we noticed repeated deviations in successive passes, which can be attributed to terrain disturbance in the form of ruts as in the area there are no distinct hills or slopes with significant degree of inclination. These tilts are compensated with TCM. For an antenna height of 3.15 m, a 1 degree tilt would lead to an antenna offset of approximately 5 cm. Contrary to the above, we observed significant discrepancies between the runs and correction services. When positioning with SF3 at the beginning of the KL path, i.e., while the tractor was moving south from under the tree cover, we observed a misalignment reaching nearly 1 m. The accuracy improved progressively after covering a distance of 10 m and remained stable until the end of the path. This was most likely caused by PPP re-convergence following losing signals of several satellites. In the case of RTK positioning, there were three large shift events, which occurred as a result of temporary losses of fix. This happened during two out of three runs on the KL path.

We observed a systematic shift of the circular path, which was consistent for all three correction services. The eastward shift measured 70 cm, while the southward shift 50 cm. The determined shifts did not match the offsets noted for the straight paths. Due to the lack of official specifications from the service provider, the analysis used the path determined by fitting a circle to the data set of measured points. The radii of the fitted circles did not differ by more than 1 cm from the predefined radius of 20 m (Figure 7). Notably, paths recorded under different correction services were aligned with each other, with a differences range from -4 cm to +5 cm. Again, we observe repeated deviations resulting from the roughness of the terrain.

Throughout the experiment, DOP parameters, PDOP in particular, were the sole indicators of the quality of the GNSS positioning. However, we found no clear correlation between the PDOP values and the internal accuracy of the determined positions (Figure 8). In autosteering mode, the highest PDOP value of 2.9 was recorded with SF1 on the KL path, yet the distances still fell within the range of 5 to 10 cm. For the other two services, the PDOP values did not exceed 2.6 in that location. At PDOP below 1.5, errors showed both sub-5 cm as well as significantly larger values, exceeding 20 cm.

The overall evaluation of correction services (Figure 9) reveals that horizontal precision of less than 2 cm (1 sigma uncertainty) was achieved in either open-sky or partially obstructed conditions. However, for the IJ and KL paths, precision was significantly degraded, as discussed in previous sections. Due

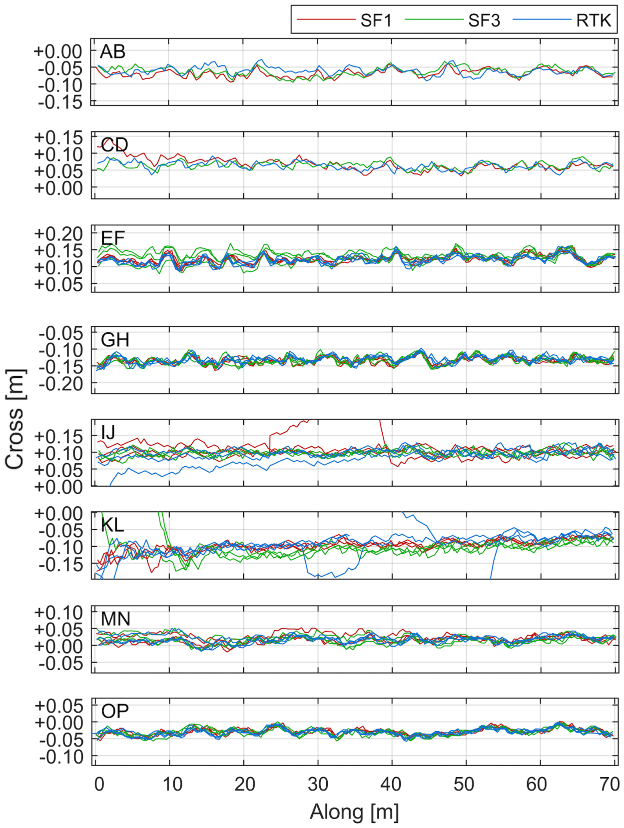

Figure 6. Deviations of GNSS positions from the predefined straight paths

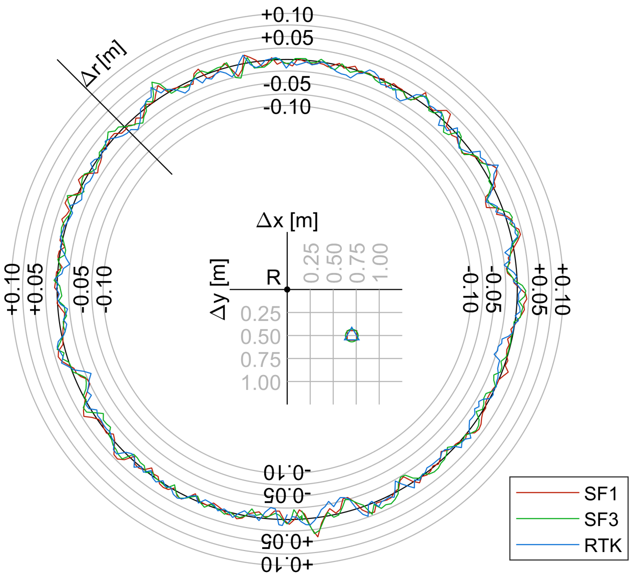

Figure 7. Deviations of GNSS positions from the fitted circular path; horizontal offset between the predefined center of the circle and fitted circle centers are indicated inside the plot

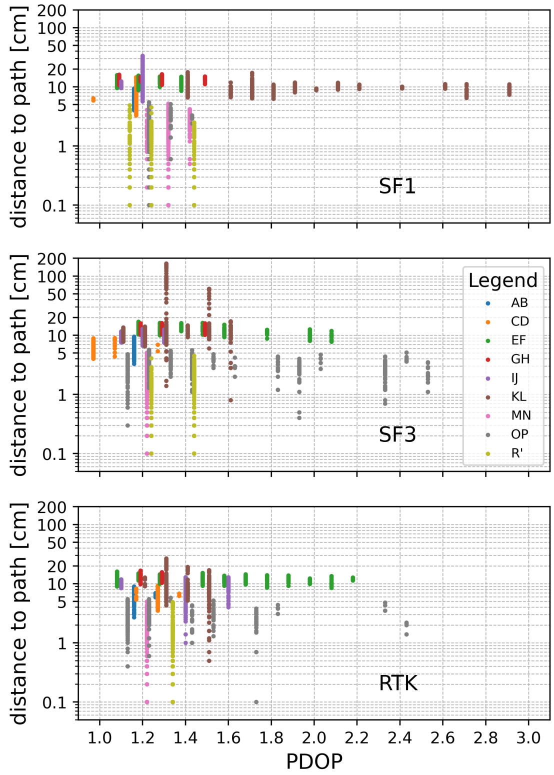

Figure 8. Internal accuracy of SF1 (top), SF3 (middle) and RTK (bottom) with respect to PDOP

to the offset of circular paths, the accuracy with respect to the R circle was highly compromised. Nevertheless, after removing the offset, sub-centimeter level precision was maintained. All correction services resulted in similarly accurate positioning ranging from 2 cm for the MN path to 13 cm for the GH path, except for the SF3 service and KL path, for which the accuracy exceeded 30 cm. The maximum errors were typically within the 5 cm to 15 cm range, with some outliers noticed for the SF1 on CD and IJ paths, as well as for the SF1 on the KL path. Notably, the accuracy, precision, and maximum error appeared to be path-specific rather than service-specific. The underperformance of the SF3 service on path KL in comparison to the other two correction services was due to the re-initialization of the PPP filter.

3.3 External Validation

The external validation was conducted by analyzing the coordinates obtained through total station measurements. Although the retroreflector was shifted with respect to the GNSS antenna: we ignore the vertical offset, since the vertical component was not considered in our analysis, and the offset of 15cm did not affect the horizontal component significantly when driving on a flat terrain; we ignore the horizontal offset, because the retroreflector aligned with the tractor's axis of symmetry, thus following the GNSS antenna while driving.

On average, we measured 72 points for each pass. The repeating gap in the MN path was caused by the temporary loss of prism visibility by the total station, attributed to the tripod set up at the P2 point. We noticed that the points measured during auto-guidance with both Starfire services (SF1, SF3) were significantly shifted from the defined paths, which was not the case for the RTK. Missing time stamps for total-station measurements allowed us to determine only the offset parallel

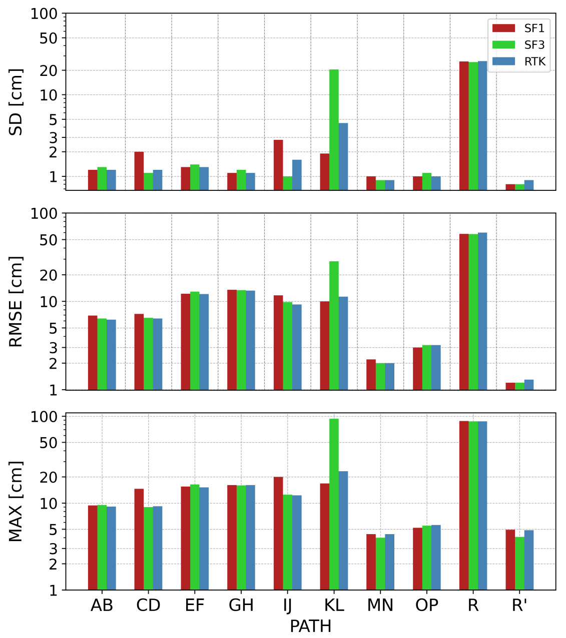

Figure 9. Precision (top), accuracy (middle), and maximum error (bottom) of GNSS coordinates with respect to the predefined paths (internal validation)

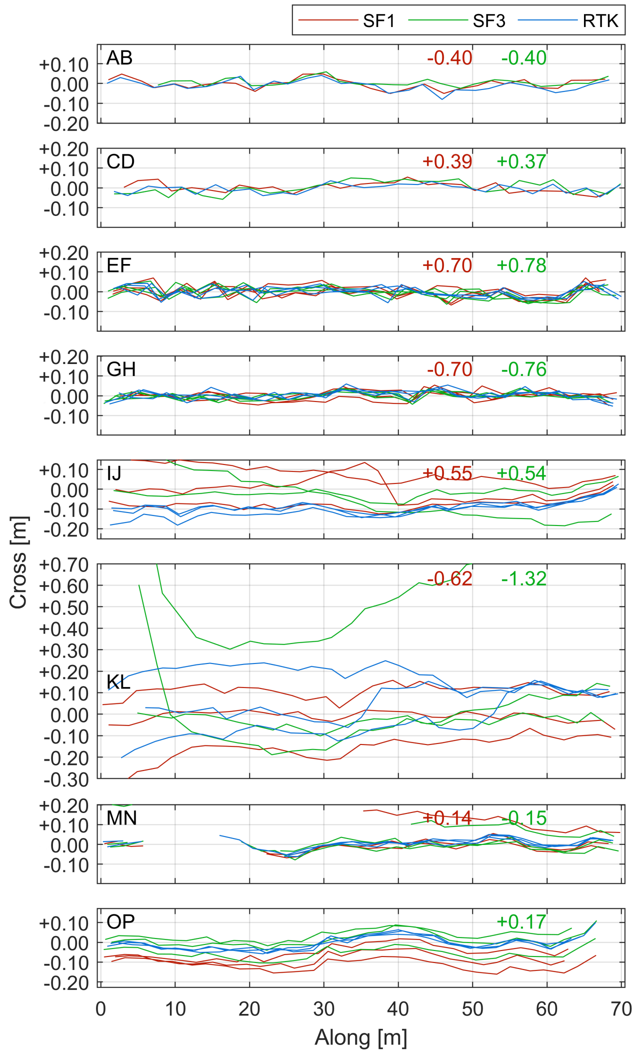

Figure 10. Deviations of positions determined by the total station from the predefined straight paths; values in the top right corner indicate offset applied for each correction service to align the measurements with the predefined path

to the corresponding path, leaving the along-track offset unknown. This was an obstacle in checking whether the offsets resulted from an incorrectly defined reference frame. However, we noticed that offsets were area-specific, i.e., they were similar for parallel paths and well-aligned between the two Starfire services. The magnitude of the offsets ranged from −1.32 m (SF3, KL path) to +0.78 m (SF3, path EF). After removing the offsets, all passes and paths aligned together (Figure 10), indicating the high precision of all three correction services. Due to unsynchronized surveying combined with the lower interval of measurements, approximately every 1 m, the terrain disturbances were not as clearly noticeable as in Figure 6. For the KL path, the accuracy and precision were the lowest compared to other straight paths, and with the SF3 service, there was a clear disagreement between the consecutive runs, which we justified by the re-initialization of the PPP solution.

Similar to internal validation, we observed a systematic shift of the circular path. However, this time the shift was service-specific: the eastward offsets equalled 0.33 m, 0.25 m, and 0.82 m for SF1, SF3, and RTK, respectively, whereas the corresponding readings for the southward shift were 0.73 m, 0.90 m and 0.39 m. Upon removing the offsets, the deviations of the measured positions with respect to the fitted circle remained within a range of −10 cm to +2 cm (Figure 11). The measured circles were of a smaller radius (by approximately 5 cm) than the one pre-defined. Such systematic effect can be attributed to the tilt of the tractor while turning combined with the offset location of the retroreflector relative to the GNSS antenna.

We used consecutive runs over selected straight paths to verify the pass to pass accuracies declared by service provider (Table 2). The pass-to-pass errors were calculated as point-to-line distances, taking all points from the first and the third run, while the line was formed by the points acquired in the second run. We determined Cumulative Distribution Function (CDF) for each correction service and path (Figure 12). We observed the consistency of CDFs among correction services on paths located in an area with open-sky conditions (EF, GH). For both paths and every correction service, 95% of distances ranged from 2.5 cm to 4.5 cm. Nevertheless, as the tractor approached the forest, we observed a rapid increase in the pass-to-pass error and the claimed 95% accuracy was no longer achieved. We noticed the extreme underperformance of SF3 service, for which the accuracy was 54.5 cm and 65.6 cm on the IJ and KL paths, respectively. Once the tractor left the highly obstructed area, and reached paths MN and OP, the performance of correction services improved, except the SF1 service on path MN. Typically, the accuracy for RTK was the highest, but it only conformed with the declared ±2.5 cm accuracy solely on the last two paths. SF3 achieved the claimed 95% accuracy only once (GH path), while SF1 underperformed only in the more challenging environments (paths KL and MN).

The overall statistics for the external validation provide additional findings with respect to internal validation (Figure 13). The precision varied among services and was typically the highest for RTK. While SF3 was slightly more precise than SF1 in open-sky or partially obstructed conditions, it was vulnerable to temporal losses of GNSS signals, leading to the re-initialization of the PPP solution, thus degradation of positioning (along paths IJ and KL). Yet, under favorable conditions, precision better than 3 cm was achieved. The accuracy of SF1 and SF3 was much lower than that of the RTK, due to significant biases. For RTK the accuracy was in general higher than

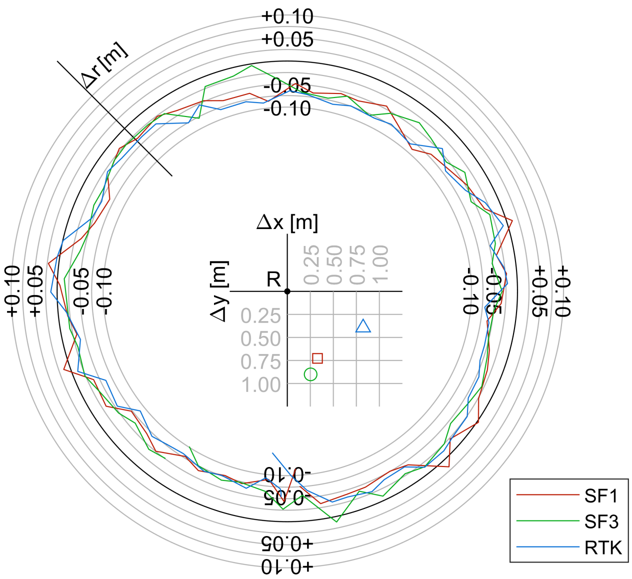

Figure 11. Deviations of positions determined by the total station from the fitted circular path; horizontal offset between the predefined center of the circle and fitted circle centers are indicated inside the plot

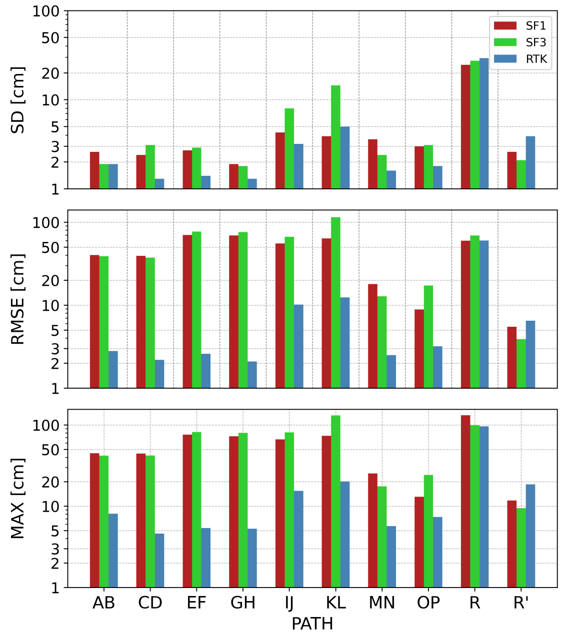

Figure 13. Precision (top), accuracy (middle), and maximum error (bottom) of positions determined by the total station with respect to the predefined paths (external validation)

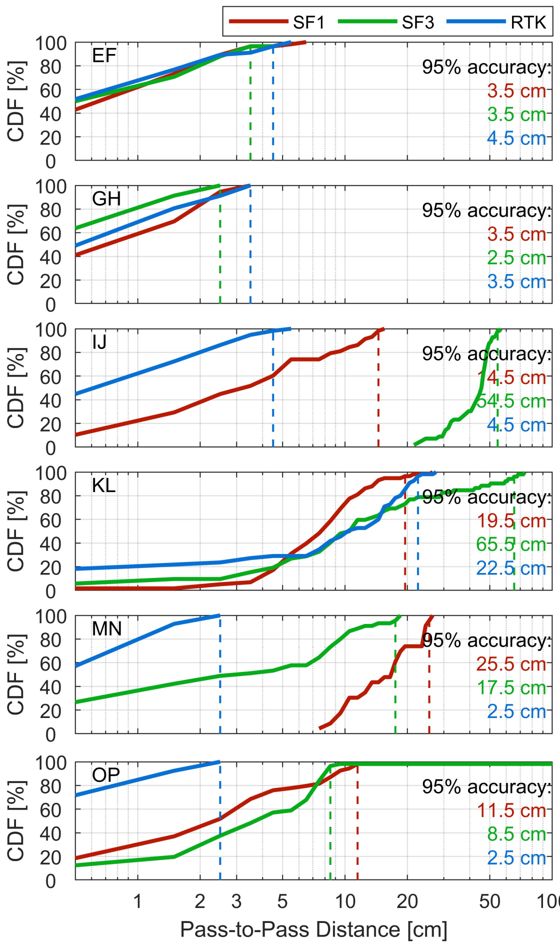

Figure 12. Cumulative distribution functions (CDF) of pass-to-pass distances for each path and correction service; vertical lines indicate 95% accuracy level

5 cm, with individual errors reaching up to 8 cm and 20 cm on straight and circular paths, respectively. For paths IJ and KL the RTK accuracy degraded to approximately 10 cm, with a maximum error of 20 cm.

4 Conclusion

The study highlights differences in the performance of the three GNSS correction services for PA under both favourable and challenging conditions. Classical surveying serves independent reference data, allowing for a reliable comparative analysis. Although we found no correlation between position accuracy and precision with PDOP, the distinct performance of the correction services implies that environmental factors play a huge role in achieving desired precision and accuracy of GNSS positioning in PA. The external validation reveals that tractor trajectories with SF1 and SF3 services are shifted with respect to predefined straight paths, which is not the case for RTK. Offsets of up to several decimeters are service- and area-specific, indicating a major issue with the stability of the reference frame. Offsets are also present for the circular path and all three correction services, which is shown by both internal and external validation. Further investigations are required to understand this issue.

In terms of precision, the SF1 service outperforms the manufacturer's reports on various paths, providing results similar to SF3 in open-sky operations and avoiding major underperformance in more challenging environments. Conversely, the SF3 service proves less reliable in highly-obstructed terrains, which is typical for PPP-based positioning. RTK emerges as a service that demonstrates consistent performance, providing the most precise determination of position, with only occasional, modest shifts. Under favourable conditions the pass-to-pass accuracy at 95% confidence level is higher than 11.5 cm, 8.5 cm, and 4.5 cm for SF1, SF3, and RTK, respectively. In the worst-case scenario, the corresponding accuracy is 25.5 cm, 65.5 cm, and 22.5 cm. While all three correction services often exceed pass-to-pass accuracy at 95% confidence level, we cannot question their nominal performance. Not only our experiments were performed in challenging environments, but also the results are slightly contaminated by the tractor tilt. It is the ground position that is important for the PA applications, while we analyze positions of the GNSS antenna and the retroreflector located on the tractor roof. In practice, the terrain compensation module takes into account GNSS position, its vertical offset and tilt, further enhancing the ground trajectory.

Future research should identify the source of coordinate offsets, ideally, in cooperation with the service provider. Moreover, terrain-dependent positioning accuracy should be investigated, including an examination of various services used in PA applications. This could involve increasing the number of test runs and their frequency, also in less conventional scenarios such as spiral trajectories, in order to contribute to a more comprehensive understanding of the strengths and limitations of different positioning services. Adjusting the automated guidance system settings and machine speed can also play a crucial role in achieving more accurate results. This could potentially impact the advancement of positioning solutions for various applications in PA and beyond.

Acknowledgments

The authors acknowledge "Agripuls Wiesław Kowalczyk" for providing the tractor equipped with the Starfire 6000 receiver for the time of experiment. The authors declare that they have no known competing financial interests or personal relationships that could have appeared to influence the work reported in this paper.

References

Adamchuk, V. I. (2008). Satellite-based auto-guidance. University of Nebraska at Lincoln Extension Circular, EC706, Lincoln, Nebraska, on-line, Last accessed: 2023.12.

Bak, T. and Jakobsen, H. (2004). Agricultural robotic platform with four wheel steering for weed detection. *Biosystems Engineering*, 87(2):125–136, doi:10.1016/j.biosystemseng.2003.10.009.

Bell, T. (2000). Automatic tractor guidance using carrier-phase differential GPS. *Computers and Electronics in Agriculture*, 25(1–2):53–66, doi:10.1016/s0168-1699(99)00055-1.

Catania, P., Comparetti, A., Febo, P., Morello, G., Orlando, S., Roma, E., and Vallone, M. (2020). Positioning accuracy comparison of GNSS receivers used for mapping and guidance of agricultural machines. *Agronomy*, 10(7):924, doi:10.3390/agronomy10070924.

Cheein, F. A. A. and Carelli, R. (2013). Agricultural robotics: Unmanned robotic service units in agricultural tasks. *IEEE Industrial Electronics Magazine*, 7(3):48–58, doi:10.1109/mie.2013.2252957.

Coyne, P., Casey, S., and Milliken, G. (2003). Comparison of differentially corrected GPS sources for support of site-specific management in agriculture. *Kansas State University. Agricultural Experiment Station and Cooperative Extension Service*.

Esau, T. J., MacEachern, C. B., Farooque, A. A., and Zaman, Q. U. (2021). Evaluation of autosteer in rough terrain at low ground speed for commercial wild blueberry harvesting. *Agronomy*, 11(2):384, doi:10.3390/agronomy11020384.

Guo, J., Li, X., Li, Z., Hu, L., Yang, G., Zhao, C., Fairbairn, D., Watson, D., and Ge, M. (2018). Multi-GNSS precise point positioning for precision agriculture. *Precision Agriculture*, 19(5):895–911, doi:10.1007/s11119-018-9563-8.

Harbuck, T. L., Fulton, J. P., McDonald, T. P., and Brodbeck, C. J. (2006). Evaluation of GPS autoguidance systems over varying time periods. In *2006 ASAE Annual Meeting, Portland, Oregon, July 9-12, 2006*, por2006. American Society of Agricultural and Biological Engineers, doi:10.13031/2013.21978.

He, L. (2022). Variable rate technologies for precision agriculture. In Zhang, Q., editor, *Encyclopedia of Smart Agriculture Technologies*, page 1–9. Springer International Publishing, doi:10.1007/978-3-030-89123-7_34-2.

Huisman, L. and de Ligt, H. (2023). Validation of reference frame consistency of GNSS service products. In *International Association of Geodesy Symposia*. Springer Berlin Heidelberg, doi:10.1007/1345_2023_232.

Huuskonen, J. and Oksanen, T. (2018). Soil sampling with drones and augmented reality in precision agriculture. *Computers and Electronics in Agriculture*, 154:25–35, doi:10.1016/j.compag.2018.08.039.

Huyghebaert, B., Dubois, G., Defays, G., Namur, C. D., and Gembloux, B. (2013). Actual and global precision of the guidance system AutoTrac from John Deere. In *EFITA-WCCA-CIGR Conference, Sustainable Agriculture through ICT innovation, Turin, Italy, 2013*.

International Organization for Standardization (2010). Tractors and machinery for agriculture and forestry – test procedures for positioning and guidance systems in agriculture (ISO Standard No. 12188-1:2010). https://www.iso.org/standard/51271.html.

Karaim, M., Elsheikh, M., and Noureldin, A. (2018). GNSS error sources. In *Multifunctional Operation and Application of GPS*. InTech, doi:10.5772/intechopen.75493.

Kee, C., Parkinson, B. W., and Axelrad, P. (1991). Wide area differential GPS. *Navigation*, 38(2):123–145, doi:10.1002/j.2161-4296.1991.tb01720.x.

Keicher, R. and Seufert, H. (2000). Automatic guidance for agricultural vehicles in Europe. *Computers and Electronics in Agriculture*, 25(1–2):169–194, doi:10.1016/s0168-1699(99)00062-9.

Kim, J. H., Moon, H. C., Woo, H. J., Zhe, H. X., Kim, H. J., Kim, Y. J., and Kye, J. E. (2013). Auto-guidance system for tillage tractor. In *2013 13th International Conference on Control, Automation and Systems (ICCAS 2013)*. IEEE, doi:10.1109/iccas.2013.6704165.

Lange, A. F. and Peake, J. (2020). Precision agriculture. In Morton, Y., Diggelen, F., Spilker, J., Parkinson, B. W., Lo, S., and Gao, G., editors, *Position, Navigation, and Timing Technologies in the 21st Century*, page 1735–1747. Wiley, doi:10.1002/9781119458555.ch56.

Luck, J., Pitla, S., Shearer, S., Mueller, T., Dillon, C., Fulton, J., and Higgins, S. (2010). Potential for pesticide and nutrient savings via map-based automatic boom section control of spray nozzles. *Computers and Electronics in Agriculture*, 70(1):19–26, doi:10.1016/j.compag.2009.08.003.

Mawardi, M., Nugraheni, P., Sutiarso, L., Virgawati, S., and Fuadi, M. (2018). Mapping the Variable-Rate Application (VRA) of precision fertilizing for soybean. *Journal of Advanced Research in Applied Mechanics*, 51(1):1–9.

Montenbruck, O., Steigenberger, P., and Hauschild, A. (2020). Comparing the 'Big 4' – a user's view on GNSS performance. In *2020 IEEE/ION Position, Location and Navigation Symposium (PLANS)*. IEEE, doi:10.1109/plans46316.2020.9110208.

Onyango, C. M., Nyaga, J. M., Wetterlind, J., Söderström, M., and Piikki, K. (2021). Precision agriculture for resource use efficiency in smallholder farming systems in Sub-Saharan Africa: A systematic review. *Sustainability*, 13(3):1158, doi:10.3390/su13031158.

Perez-Ruiz, M., Slaughter, D. C., Gliever, C., and Upadhyaya, S. K. (2012). Tractor-based Real-time Kinematic-Global Positioning System (RTK-GPS) guidance system for geospatial mapping of row crop transplant. *Biosystems Engineering*, 111(1):64–71, doi:10.1016/j.biosystemseng.2011.10.009.

Pini, M., Marucco, G., Falco, G., Nicola, M., and De Wilde, W. (2020). Experimental testbed and methodology for the assessment of RTK GNSS receivers used in precision agriculture. *IEEE Access*, 8:14690–14703, doi:10.1109/access.2020.2965741.

Radočaj, D., Plaščak, I., and Jurišić, M. (2023). Global Navigation Satellite Systems as state-of-the-art solutions in precision agriculture: A review of studies indexed in the Web of Science. *Agriculture*, 13(7):1417, doi:10.3390/agriculture13071417.

Reid, J. F. and Searcy, S. W. (1987). Automatic tractor guidance with computer vision. *SAE transactions*, 96:673–693.

Schönemann, E. (2014). *Analysis of GNSS raw observations in PPP solutions*. PhD thesis, Technische Universität Darmstadt.

Stombaugh, T. (2018). *Satellite-based Positioning Systems for Precision Agriculture*, page 25–35. American Society of Agronomy and Soil Science Society of America, doi:10.2134/precisionagbasics.2017.0036.

Teunissen, P. J. G. and Khodabandeh, A. (2015). Review and principles of PPP-RTK methods. *Journal of Geodesy*, 89(3):217–240, doi:10.1007/s00190-014-0771-3.

Tran, H. T., Cao, W., Reutemann, M., Dai, L., Ostermeier, R., and Kormann, G. (2020). GNSS positioning and navigation - a foundational element of digital farming. In *2020 European Navigation Conference (ENC)*. IEEE, doi:10.23919/enc48637.2020.9317529.

Zabalegui, P., De Miguel, G., Perez, A., Mendizabal, J., Goya, J., and Adin, I. (2020). A review of the evolution of the integrity methods applied in GNSS. *IEEE Access*, 8:45813–45824, doi:10.1109/access.2020.2977455.

Zumberge, J. F., Heflin, M. B., Jefferson, D. C., Watkins, M. M., and Webb, F. H. (1997). Precise point positioning for the efficient and robust analysis of GPS data from large networks. *Journal of Geophysical Research: Solid Earth*, 102(B3):5005–5017, doi:10.1029/96jb03860.